Mesofrequency dynamic hysteresis in thin ferromagnetic films

2004 J. Phys.: Condens. Matter 16 R1369

(http://iopscience.iop.org/0953-8984/16/46/R03)

INSTITUTE OF PHYSICS PUBLISHING JOURNAL OF PHYSICS: CONDENSED MATTER

J. Phys.: Condens. Matter **16** (2004) R1369–R1386 PII: S0953-8984(04)83482-9

TOPICAL REVIEW

Mesofrequency dynamic hysteresis in thin ferromagnetic films

T A Moore and J A C Bland

Cavendish Laboratory, University of Cambridge, Cambridge CB3 0HE, UK

E-mail: jacb1@phy.cam.ac.uk

Received 9 July 2004, in final form 15 September 2004
Published 5 November 2004
Online at stacks.iop.org/JPhysCM/16/R1369
doi:10.1088/0953-8984/16/46/R03

Abstract

The spectrum of timescales for thin film magnetization reversal processes from 10^3 to 10^{-15} s is reviewed as well as appropriate experimental techniques for their investigation. The present review is motivated by the fact that most studies of magnetization dynamics have used polycrystalline NiFe thin films, whilst the magnetization dynamics of epitaxial Fe thin films, in contrast, have been little investigated, especially in the mesofrequency range (10^{-1}–10^{-6} s). Here, the competition between domain nucleation and domain wall propagation reversal processes results in a rich variety in the dynamical behaviour. We review the results of our time-resolved magneto-optic Kerr effect measurement of the dynamic hysteresis loop in epitaxial Fe thin films. Coercivity as a function of applied field frequency $H_c(f)$ is measured from the dynamic hysteresis loop in the frequency range ∼0.03–3000 Hz, corresponding to experimental timescales $t_{exp} \approx H_c/\dot{H}$ in the range $\sim 10^{-1}$–10^{-6} s, where $\dot{H}$ is the applied field sweep rate at the static coercive field H_c. Not only are two distinct dynamic regimes for $H_c(f)$ found to arise in the experimental timescale range 10^{-1}–10^{-6} s, but also the reversal processes of domain nucleation and wall propagation are seen to compete at the crossover between the two dynamic regimes, so determining the behaviour of $H_c(f)$. This review gives a historical overview of dynamic hysteresis in the mesofrequency range, and surveys recent theoretical descriptions and experiments. It is demonstrated that dynamic hysteresis experiments on thin ferromagnetic films are richly informative of the magnetization dynamics in the mesofrequency range. Methods for the interpretation of dynamic coercive field measurements $H_c(f)$ are highlighted, including an adaptation of an existing model of magnetization reversal dynamics in ultrathin magnetic layers.

(Some figures in this article are in colour only in the electronic version)

Contents

1. Introduction

The dynamics of magnetization reversal in magnetic materials is now a broad and highly active subject of research. In particular, at the present time there is a strong interest in spin dynamics in confined magnetic structures [1, 2], which include nanometre-thin single layers and multilayers as well as laterally defined submicron-scale elements. These studies are motivated by the potential applications in ultrafast switching devices such as magnetic random access memory and magnetic sensors as well as by the possibility of uncovering new physical behaviour, as seen in recent current-induced switching studies. In this work we review the present understanding of magnetization reversal dynamics in thin ferromagnetic films as revealed by mesofrequency ($\leqslant$1 MHz) dynamic hysteresis loop measurements. This experimental technique involves the application to a thin film sample of a sinusoidal magnetic field of variable frequency typically extending to kilohertz, and a measurement of the sample magnetization using the magneto-optic Kerr effect (MOKE). In this frequency range the domain wall propagation and domain nucleation processes compete to give a rich variety in the reversal dynamics.

To introduce the extensive field of magnetization reversal dynamics, we show in figure 1 the timescale and corresponding frequency range on which magnetization dynamics can occur, as well as the various experimental techniques for probing these dynamics and the types of reversal mechanism which can be expected across the timescale spectrum. For a thin ferromagnetic film, there are characteristic timescales for the attempt frequency f_0, the rate at which a small group of magnetic moments try to reverse their orientation, and for the minimum spin relaxation time $\tau_{\min}$, the shortest time for spins to stabilize after excitation over the energy barrier to reversal (occurs at critical damping, when the damping parameter $\alpha \sim 0.01$ [3]). The attempt frequency is in the range 10 MHz–1 GHz [4], and enters in the Arrhenius–Néel equation

$$\tau = \left(\frac{1}{f_0}\right) \exp\left(\frac{\Delta E}{kT}\right), \tag{1}$$

(where ΔE is the relevant energy barrier to reversal, k is the Boltzmann constant and T is the temperature) to determine characteristic reversal times τ for both nucleation of domains and depinning of domain walls, according to the energy barrier involved. The minimum spin relaxation time was calculated by Kikuchi for a molybdenum permalloy film to be of the order of 1 ns [3]. Meanwhile the theoretical limit to spin dynamics is of the order of 10 fs: this is the computed time for demagnetization after the simulated excitation of a spin system by a femtosecond laser pulse [5].

Depending on the geometry of the magnetic structure and the method of inducing magnetization reversal, different reversal processes dominate at different timescales.

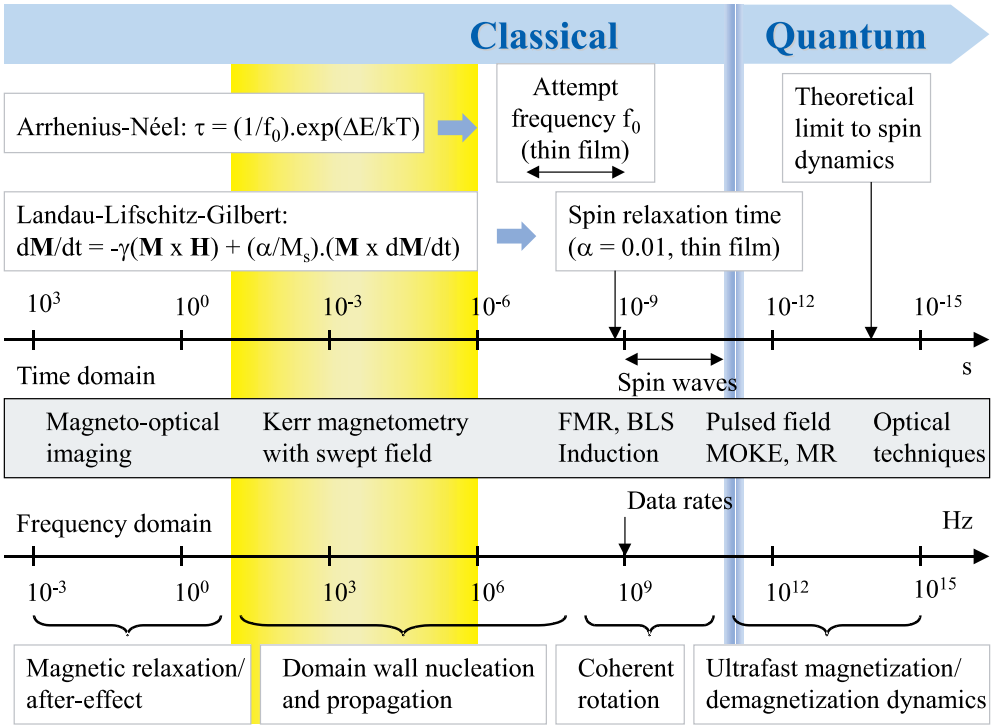

Figure 1. Timescales in magnetization dynamics, the various experimental techniques for probing these dynamics, and the types of reversal mechanism which can be expected across the timescale spectrum.

A wide range of experimental techniques is therefore required both to excite the magnetization dynamics and to probe them across the broad spectrum of timescales involved. Magnetic relaxation describes the nucleation and Barkhausen-like propagation of domain walls on the timescale of seconds in thin films subject to a constant applied field. Magnetization as a function of time is often measured by magneto-optics, either in the form of a relaxation curve or by capturing successive images of the evolving domain pattern [6, 7]. Domain wall nucleation and propagation can take variable amounts of time from large fractions of a second to microseconds, and can typically be speeded up by changing the applied field strength. The magnetization as a function of time can be conveniently measured by Kerr magnetometry, for example. If a single domain state is energetically preferred, coherent rotation is the main reversal mechanism and occurs on timescales 100 ns–100 ps. Application of a pulsed field and measurement of magnetization by induction [8], ultrafast time-resolved magneto-optic Kerr effect [9] or magnetoresistance [10] enables the examination of coherent rotation/spin precession dynamics. Meanwhile ferromagnetic resonance (FMR) experiments [11, 12] allow a measure of the spin resonance frequency, and Brillouin light scattering (BLS) [13, 14] can give information on the frequencies of collective modes of spin excitation, typically in the range 1–100 GHz. At around 10 ps, electron excitations cannot be ignored, and the Landau–Lifschitz Gilbert equation becomes invalid as quantum effects appear [15]. In the quantum regime, optical techniques are currently used to achieve ultrafast demagnetization [16]. One method is to use a femtosecond laser pulse to heat electrons in a ferromagnet above the Curie temperature within tens of femtoseconds.

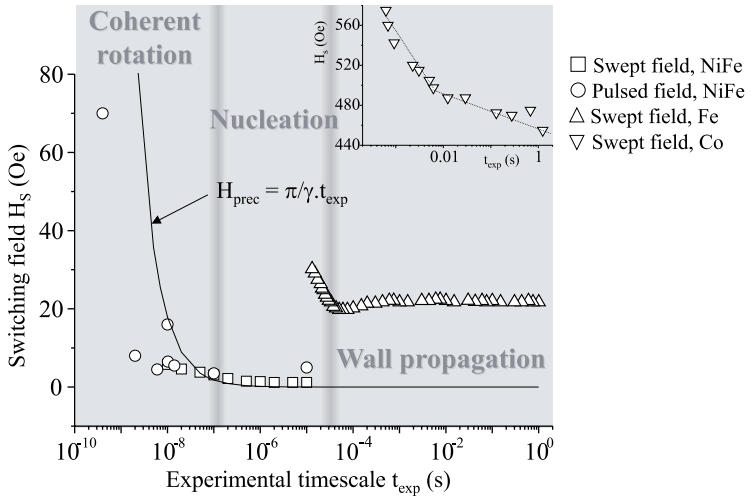

Figure 2. Collected measurements of switching fields H_S as a function of experimental timescale t_{exp} for NiFe, Fe and Co thin films. The measurements were made using either a pulsed field or a swept field to precipitate the magnetization reversal. Squares: swept field, NiFe, [20]; circles: pulsed field, NiFe, [21–24]; upright triangles: swept field, Fe, [25]; inverted triangles: swept field, Co, [17]. The solid curve corresponds to the field H_{prec} necessary to switch a magnetic moment by precession on the timescale of t_{exp}. γ is the gyromagnetic ratio.

The highlighted band of timescales from 10^{-1} to 10^{-6} s in figure 1 is the relatively unexplored region that we will concentrate on in this review of dynamic hysteresis in thin ferromagnetic films. In this mesotemporal range, domain wall nucleation and propagation are the important reversal mechanisms, and they compete for dominance to produce a rich variety in the resulting magnetization dynamics. In particular, we will discuss the crossover from propagation-dominated to nucleation-dominated reversal that is observed as the reversal time is decreased [17, 18]. There are two distinct ways to speed up reversal using an applied field. One is to apply a field pulse of larger magnitude, and the other is to apply a swept field of larger rate of change. The results of these two methods—pulsed and swept fields—can be compared by transposing to a common 'experimental timescale' t_{exp}, or the time for which the external magnetic field is applied to a sample. Such a time t_{exp} is self-explanatory in the case of a pulsed field, where the field is maintained at a constant value for a given time. However, it may also be defined for a swept-field experiment [19]:

$$t_{exp} \approx \frac{H_c}{\dot{H}}. \tag{2}$$

Here, H_c is the 'static' coercive field of the sample and $\dot{H}$ is the time rate of change of the applied field. Equation (2) defines t_{exp} as the characteristic time for the applied field to sweep through the coercive point.

Figure 2 summarizes measurements of the switching field H_S as a function of experimental timescale t_{exp} for NiFe, Fe and Co thin films. The majority of work is on NiFe polycrystalline films and laterally confined structures (square and circle symbols in figure 2), and it is seen that until $t_{exp} \leqslant 100$ ns, the switching field remains at the static value of a few Oe. At $t_{exp} \sim 10$ ns and below, a higher field is needed because the reversal is being attempted on the timescales for spin precession. The available data follow quite closely the curve for the field required to switch a magnetic moment by precession on the timescale t_{exp}, which increases rapidly at

around $t_{exp} = 10$–100 ns:

$$H_{prec} = \frac{\omega}{\gamma} = \frac{\pi}{\gamma t_{exp}}. \tag{3}$$

Here, γ is the gyromagnetic ratio and the field pulse is terminated after half the precession period, i.e. $t_{exp} = T/2$.

Compared to polycrystalline NiFe, there has been little work on epitaxial Fe and Co thin films. In Fe (upright triangle symbols), the static coercivity is several times larger than in NiFe, and the switching field starts to increase at $t_{exp} \sim 30$ μs. In Co (inverted triangles), there is an abrupt change of slope at an even larger value of t_{exp} ($\sim$5 ms), and in addition the switching field increases gradually in the region of decreasing $t_{exp} = 1$ s $\rightarrow$ 5 ms, rather than remaining at a constant 'static' value. In this review, we will discuss studies of switching field in epitaxial Fe films grown on GaAs(001) in the range $t_{exp} \sim 10^{-1}$–10^{-6} s accessible by our dynamic hysteresis measurement.

The review will be presented largely in chronological order. In section 2, studies of dynamic hysteresis in various magnetic materials, conducted before the 1980s and as far back as the end of the nineteenth century, will be presented. Section 3 discusses the theoretical descriptions of dynamic hysteresis developed in the 1990s, including scaling laws. Section 4 concentrates on the experimental works from the early 1990s and on, whilst in section 5 recent experiments and analyses are discussed. Before concluding, section 6 mentions some related and applications-oriented research.

2. Historical overview

Experiments to measure dynamic hysteresis loops are generally performed by applying a sinusoidal external field and changing either the field amplitude or frequency. There have been several studies of the amplitude and frequency dependence of hysteresis loops in bulk materials [26, 27], some dating back one hundred years or more [28–30]. Perhaps the earliest and best known descriptions of amplitude-dependent hysteresis in iron are given by the Rayleigh and Steinmetz power-laws:

$$W_H \approx B_m^3, \tag{4}$$

$$W_H \approx B_m^{1.6}. \tag{5}$$

Here, W_H is the area of the hysteresis loop and is a measure of the energy dissipated into the system per cycle (erg cm^{-3}). The Rayleigh law [26, 31] (equation (4)) applies for low values of maximum induction B_m, while the Steinmetz law [26, 28, 30] (equation (5)) applies for values of B_m in the range 500–15 000 G. A wide variety of soft magnetic materials, including cobalt and silicon–iron as well as permalloy, satisfy the Steinmetz law.

Ewing and Klaassen discussed the frequency dependence of hysteresis loops in soft iron [28, 29]. Figure 3 shows the hysteresis loops of a soft iron bar at various frequencies, with the amplitude fixed. As the frequency was increased, it was found that the area of the loop increased at first, and eventually decreased.

Extensive studies of the frequency dependence of hysteresis loops in ferrites were made by Smit and Wijn in the 1950s [27]. It was found that ferrites with a high initial permeability ($\mu_i > 400$) have frequency-dependent magnetization curves for frequencies below the ferromagnetic resonance frequency. Metallic magnets have a different frequency response from insulating magnets such as ferrites because they experience eddy current losses. The total energy loss in a magnetic system per cycle is often expressed as the sum of the components

$$W_{tot} = W_H + W_{ec} + W_a, \tag{6}$$

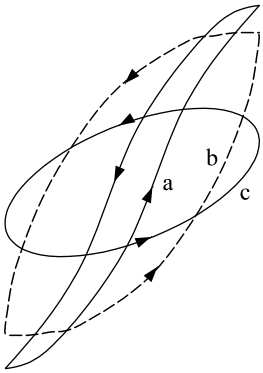

Figure 3. Hysteresis loops for a soft iron bar for various frequencies of the applied field: (a) cycle performed slowly, (b) period = 3 s, (c) period = 0.43 s (after [28, 29]).

where W_H is the hysteresis loss, W_{ec} the eddy current loss and W_a the anomalous loss (discrepancy between the measured loss and the loss expected from the sum of hysteresis and eddy current losses). The losses in metallic magnetic materials such as silicon-iron and permalloy have been well characterized due to the demand for high performance transformer cores.

In thin magnetic films eddy currents are difficult to initiate due to the reduced dimensions, and the hysteresis losses dominate. Thin films are thus an ideal system for the study of dynamic hysteresis. One of the earliest works was by Hatfield in 1965 [20], who investigated the switching of 0.5–2.0 μm-thick electrodeposited permalloy films as a function of the frequency of sinusoidal applied fields in the range 1 kHz to 1 MHz. It was found that the field required for complete flux reversal ($\sim$ coercive field) increased with frequency, and eventually exceeded the anisotropy field in the region of 150 kHz. The conclusion was that the reversal mechanism in these films changes from irreversible domain wall motion to nonuniform rotation of the magnetization. This kind of conclusion—that there may be a change of reversal mechanism as the field sweep rate is increased beyond some boundary value—is widely reached in present-day studies of dynamic hysteresis.

There were no further systematic studies of the frequency dependence of hysteresis loops in thin magnetic films until the 1990s. These studies, which will be discussed in detail in section 4, use the magneto-optic Kerr effect for the measurement of dynamic hysteresis loops. This technique typically employs a linearly polarized fixed wavelength laser source. The beam is focused to the required size on the film, and acquires a Kerr rotation and ellipticity upon reflection. Passing the reflected light through an analyser whose polarization axis is nearly crossed with that of the incident beam and onto a photodiode allows a measurement of light intensity that is proportional to the magnetization averaged across the laser spot at the film surface. A schematic of our experimental set-up, the ac Kerr magnetometer, which uses the longitudinal Kerr effect, is shown in figure 4. We use a laminated-core electromagnet to generate sinusoidally varying fields in a frequency range $\sim 0.03 < f < 3000$ Hz, which typically corresponds to experimental timescales in the range $\sim 10^{-1} > t_{exp} > 10^{-6}$ s, depending on the static coercive field of the sample (equation (2)).

The magneto-optic Kerr effect (MOKE) can be used to probe the magnetization switching dynamics because interactions of the laser light with the ferromagnetic material typically take place on a much faster timescale $\sim 10^{-15}$ s [32]. In our MOKE magnetometry experiment the limiting factor is the photodetection system, which should have a response time significantly

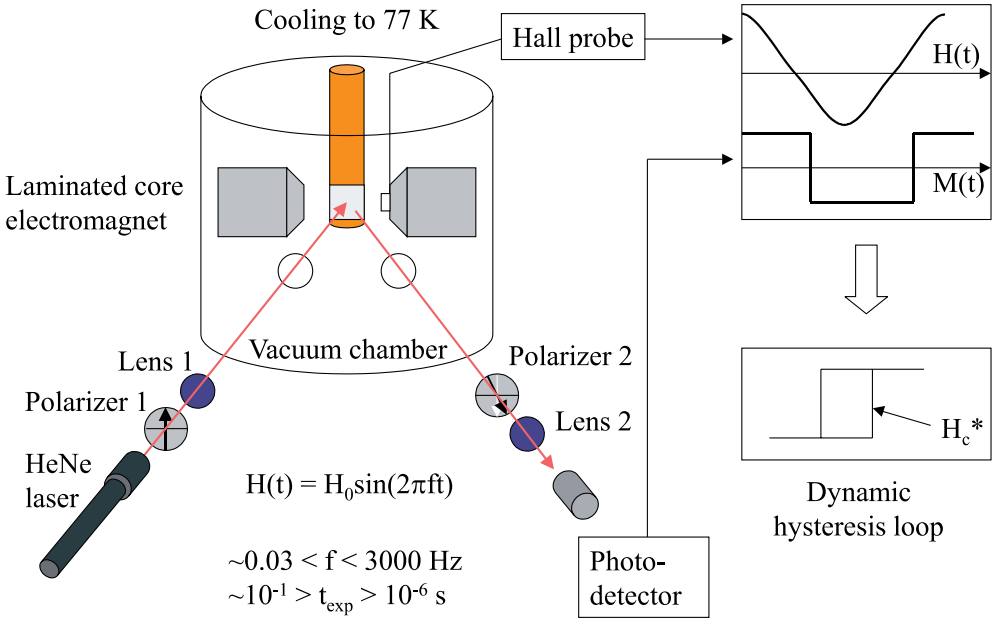

Figure 4. A schematic representation of the Cambridge ac Kerr magnetometer. The longitudinal MOKE configuration is used. A laminated-core electromagnet supplies sinusoidally varying fields with frequency extending to a few kilohertz. The thin film sample may be cooled to 77 K, in which case it is necessary to place the sample and electromagnet in a vacuum chamber to avoid condensation on the film surface. The applied field and Kerr intensity (magnetization) are recorded as a function of time and used to generate dynamic hysteresis loops.

faster than the minimum experimental timescale $\sim 10^{-6}$ s. We use an intensity stabilized HeNe laser, the beam of which is passed through a polarizer P_1 to give it an enhanced degree of linear polarization. After reflection from the sample the beam passes through an analyser P_2 with polarization axis rotated 1°–2° away from extinction. The emergent light intensity is detected by an Si avalanche photodiode (bandwidth 80 MHz, rise time 4.4 ns) mounted directly on a commercial amplifier (bandwidth 30 MHz, rise time 10 ns). Lenses L_1 and L_2 may be employed to focus the beam onto the film surface and back onto the photodiode.

If sample cooling is required the electromagnet and sample may be placed in an ultrahigh vacuum chamber to prevent the accumulation of water vapour on the film surface. The sample is attached to the end of a tube extending down inside the vacuum chamber which is filled with liquid nitrogen. Employing a cartridge heater device to offset the cooling by liquid nitrogen allows one to obtain sample temperatures in the range 77–300 K.

Plotting magnetization over one cycle as a function of applied field gives a dynamic hysteresis loop, from which the dynamic coercive field H_c^* may be obtained.

3. Theoretical descriptions

The work of Rao *et al* [33] reported in 1990 was the first attempt to understand the power-law behaviour of the area of the hysteresis loop (e.g. the Steinmetz law (equation (5))) from a microscopic point of view. Here, a 3D continuous spin system and a 2D discrete (Ising) spin system as a function of the amplitude (H_0) and frequency (f) of an external field were studied. In this, and in subsequent studies of such systems in both two and three dimensions [34–41],

Table 1. Theoretical scaling exponents for various 2D and 3D continuum (†) and Ising (‡) model systems.

Model	α	β	Reference
† 3D $(\Phi^2)^3$	2/3	1/3	[33]
† 3D $(\Phi^2)^2$	0.66	0.33	[33]
† 2D $(\Phi^2)^2$	0.47	0.40	[34]
† 2D $(\Phi^2)^2$	1/2	1/2	[38]
† 3D O(N)	1/2	1/2	[35–37]
‡ 3D	0.67	0.45	[41]
‡ 2D	0.70	0.36	[41]
‡ 2D	0.46	0.36	[39]
‡ 2D	1/2	1/2	[35, 36]
‡ 2D	2/3	2/3	[40]

the following power law emerged, holding true at both low H_0 and f:

$$A \propto H_0^{\alpha} f^{\beta}. \tag{7}$$

This power law suggests that, under the specified conditions, the area of the hysteresis loop A scales with the external field amplitude H_0 and frequency f, and it is referred to as a scaling relation. α and β are known as scaling exponents, and specific values of these are predicted by the various theoretical models (table 1). They do not represent any physical quantity; they merely describe the rate at which the hysteresis loop area grows with amplitude or frequency for the system in question.

A simplification of the scaling relation (equation (7)) was proposed by Zhong and Zhang [38]:

$$A \propto \dot{H}^{\alpha}, \tag{8}$$

where $\dot{H}$ is the applied field sweep rate. Both the scaling relations equations (7) and (8) have been used by experimentalists to fit to data and thereby to determine the exponents α and β to compare with the theoretical models [18, 42–50]. The continuum models are relevant to small, insulating, defect-free, single-domain particles with a very small magnetic anisotropy, whilst the Ising models are relevant to ferromagnetic thin films with strong uniaxial anisotropy. However, neither type of model considers domain processes.

4. Experimental background

In the last ten years, experimental studies of dynamic hysteresis in thin magnetic films have often used the power laws for loop area scaling for analysis of data [18, 42–50]. The first systematic experiments were made by He and Wang in 1993 [42]. Their results confirmed the scaling relation equation (7) proposed by Rao *et al* [33] and their scaling exponents $\alpha = 0.59 \pm 0.07$ and $\beta = 0.31 \pm 0.05$ were within experimental error consistent with the exponents $\alpha = 0.66$ and $\beta = 0.33$ determined in the theoretical study (see table 1). Further experimental studies of various continuous thin film systems [43–45] demonstrated that although the hysteresis loop area always followed one or other of the scaling relations equations (7) or (8), the scaling exponents were not always compatible with each other or with the theoretical models. The experimental scaling exponents are summarized in table 2.

It was soon realized that the power laws for loop area scaling have limited use for the interpretation of data in the context of real physical processes. For example, in the scaling of loop area with frequency, Suen *et al* noted that the scaling exponent β was larger for an

Table 2. Experimental scaling exponents in $A \propto H_0^{\alpha} f^{\beta}$ (†) and $A \propto \dot{H}^{\alpha}$ (‡) for various continuous ferromagnetic (FM) thin film systems.

System	α	β	FM layer thickness (Å)	Reference
† Fe/Au(001)	0.59	0.31	4.3	[42]
† Co/Cu(001)	0.67	0.66	2.5–7.5	[43]
† Fe/W(110)	0.25	0.06	2.1–5.6	[44]
† Co/Cu(001)	0.15	0.02	2.5–5.0	[45]
System	α_l	α_h	FM layer thickness (Å)	Reference
‡ Au/Co/Au/MoS_2	0.036	0.177	80	[17]

Fe film on a stepped W(110) surface than for the same film on a flat W(110) surface (flat surface $\beta = 0.063 \pm 0.002$, stepped surface $\beta = 0.076 \pm 0.002$) [44]. Assuming that reversal takes place predominantly by domain wall propagation, this suggested that step-induced film roughness plays a role in domain wall dynamics. Indeed, the spot size-dependent Kerr loops of Suen *et al* suggested that magnetization reversal in 2.1–5.6 Å Fe/W(110) proceeds via domains on the scale of $\sim$100 μm, and hence that the magnetization reversal dynamics are governed by domain processes. The exponents β obtained by Suen *et al* are essentially a factor of ten smaller than those predicted by the various theoretical models (see table 1). Since the models do not consider domain wall coercivity-dominated magnetization reversal processes, it is not really surprising that they are not supported by these experiments.

With the work of Raquet *et al* [17, 51] and, in our group, Lee *et al* [18, 47–49], evidence was obtained relating to a phenomenon seen much earlier by Kryder and Humphrey [21]. The loop area scaling in epitaxial Fe/GaAs(001) and Fe/InAs(001) thin films [18, 47], and in epitaxial single ferromagnetic NiFe and Co layers [48, 49] was investigated. In all cases, the hysteresis loop area A was found to follow equation (8). However, in a double logarithmic plot of dynamic coercive field H_c^* (proportional to A for saturated, easy axis loops) versus sweep rate $\dot{H}$, it was clear that the slope of the graph and hence the exponent α varied with the sweep rate (figure 5). Two distinct regions in a double logarithmic plot were seen in which approximately linear behaviour occurred but with different values of α. For the Cu/60 Å NiFe/Cu/Si single magnetic layer, for example, α was found to be $\sim$0.13 at low sweep rates and $\sim$0.70 at high sweep rates.

A similar variation of H_c^* with sweep rate $\dot{H}$ was observed in Au/8 Å Co/Au/MoS_2 sandwiches with perpendicular magnetic anisotropy by Raquet *et al* [17, 51]. In one sample, they noticed a 'drastic transition' in the variation of coercive field against sweep rate at 180 kOe s^{-1} (see figure 6 and also table 2, where α changes from α_l (low) to α_h (high) at this value of sweep rate). The main objective of [17] was to develop a model of hysteresis in ultrathin magnetic layers that accounted for dynamical effects and the competition between domain nucleation and domain wall motion. Using their expression for the magnetization as a function of magnetic field and field sweep rate, $M[H, \dot{H}]$, they made fits to their experimental hysteresis loops, allowing the parameters of Barkhausen volume, nucleation rate, domain wall velocity, critical radius of nucleated domain and total number of nuclei sites to vary. From an examination of these parameters, it was established that below $\dot{H} = 180$ kOe s^{-1} (termed the 'low dynamic regime'), the main reversal mechanism was domain wall motion. Above $\dot{H} = 180$ kOe s^{-1} (termed the 'high dynamic regime'), the nucleation rate was seen to increase and the domain wall velocity to decrease. It was suggested that, as $\dot{H}$ increases, the domain wall motion mechanism becomes less and less efficient. In the high dynamic regime, nucleation was considered to be the dominant reversal mechanism.

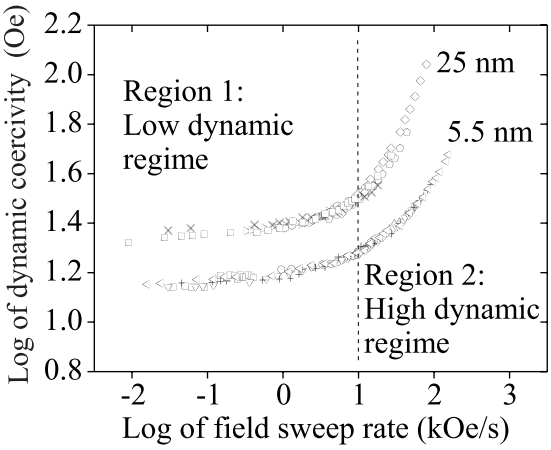

Figure 5. A double logarithmic plot of dynamic coercive field H_c^* versus applied field sweep rate $\dot{H}$ for two epitaxial Fe/GaAs(001) thin films (from [18]).

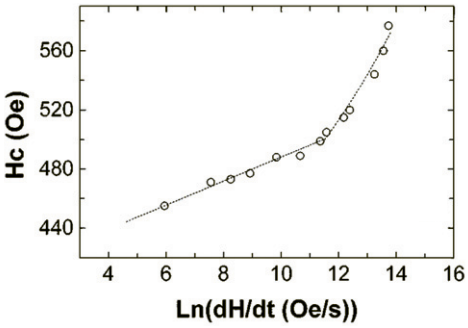

Figure 6. The coercive field H_c versus the logarithm of dH/dt for an Au/Co(0.8 nm)/Au sandwich at 300 K (from [17]).

The results of Lee *et al* for single Co and NiFe layers [48, 49], and for Fe/GaAs(001) and Fe/InAs(001) [18, 47], were qualitatively in good agreement with the experimental results and theoretical model of Raquet *et al*. Hence the differing values of the exponent α between the two distinct regions were attributed to the change of reversal mechanism from domain wall motion to nucleation with increasing sweep rate. The main difference between the results of Lee *et al* and those of Raquet *et al* was that, instead of a sharp transition from the low to the high dynamic regime, a broad transition region over a small range of sweep rate (typically 10 kOe s^{-1} for Fe/GaAs(001) thin films) occurred. This 'smoothing' effect is now understood to arise from the finite bandwidth of the experimental apparatus, and if the measurement method is refined, a sharp transition can be observed [25].

For the Fe/GaAs(001) and Fe/InAs(001) thin films [18, 47], in the low dynamic regime the values for the exponents α are a factor of ten different from those of the theoretical predictions, whereas in the high dynamic regime, the values are similar to those of the theoretical predictions (table 1). The conclusion was that the discrepancy arises because the theoretical models do not consider the domain wall motion and nucleation processes that govern the magnetization reversal dynamics in these systems.

It is useful at this point to construct a table of experimental dynamic scaling exponents in the low dynamic regime for the various continuous Fe and Co thin film systems that have been

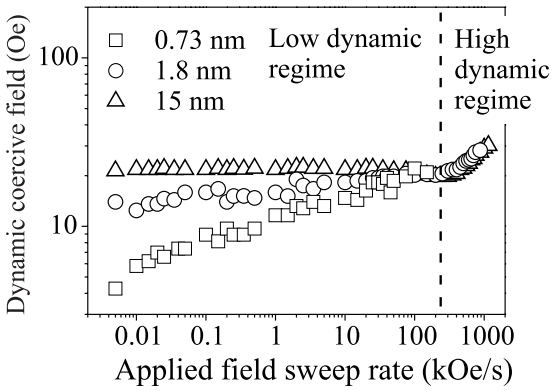

Figure 7. The dynamic coercive field H_c^* as a function of applied field sweep rate $\dot{H}$ for Fe/GaAs(001) films of varying thickness 0.73–15 nm.

Table 3. Experimental scaling exponents in the low dynamic regime for various continuous Fe and Co thin film systems.

System	Thickness (Å)	α (low $\dot{H}$)	Reference	Size
Fe/W(110)	2.1–5.6	$\alpha \sim 0.25$	[44]	Thin
Fe/Au(001)	4.3	$\alpha \sim 0.59$	[42]	Thin
Co/Cu(001)	2.5–5.0	$\alpha \sim 0.15$	[45]	Thin
Co/Cu(001)	2.5–7.5	$\alpha \sim 0.67$	[43]	Thin
Au/Fe/GaAs(001)	55, 250	0.04	[18]	Thick
Au/Fe/InAs(001)	150	0.02	[47]	Thick
Cu/Co/Cu/Si(001)	40	0.02	[48]	Thick
Au/Co/Au/MoS_2	80	0.036	[17]	Thick

investigated (table 3). These data suggest that scaling exponents in the low dynamic regime are generally an order of magnitude larger for the thin films ($\sim$ few ångströms) than for the thick films ($\sim$15 Å and beyond). The data provided a motivation for the investigation of thickness-dependent dynamic hysteresis scaling [25]. In this study, frequency-dependent hysteresis loops were measured for Fe/GaAs(001) thin films with Fe thickness ranging from 7.3 to 150 Å. A similar series of Fe/InAs(001) films was also investigated, with a view to determining the effect of the contrasting anisotropy strengths and symmetries [52–54]. In accordance with the work of Lee *et al*, two distinct regions in a double logarithmic plot of dynamic coercive field H_c^* versus field sweep rate $\dot{H}$ were seen in which approximately linear behaviour occurred but with different values of α (see figure 7). A transition at 250 kOe s^{-1} separated these two regions for all films. In the low dynamic regime α was found to be a decreasing function of Fe film thickness (see figure 8). It is seen that α varies on a lengthscale of the order of the exchange length d_{ex}, where $d_{ex} \approx 50$ Å in Fe. This thickness dependence suggests that the interface controls the dynamic coercive field variation with frequency in the low dynamic regime, and it is expected that this is via domain wall pinning arising from interface roughness. Interface roughness-induced pinning sites are expected to trap domain walls more effectively at reduced film thickness [55]. Evidence for such pinning sites in 55 Å Fe/GaAs(001), spatially distributed on a lengthscale of a few hundred microns, has been inferred from Kerr microscopy studies [18]. The values of α in the low dynamic regime for the Fe/InAs(001) films were similar to those for the Fe/GaAs(001) films of comparable thickness ($\sim$20 Å Fe, $\alpha \sim 0.05$; $\sim$55 Å Fe,

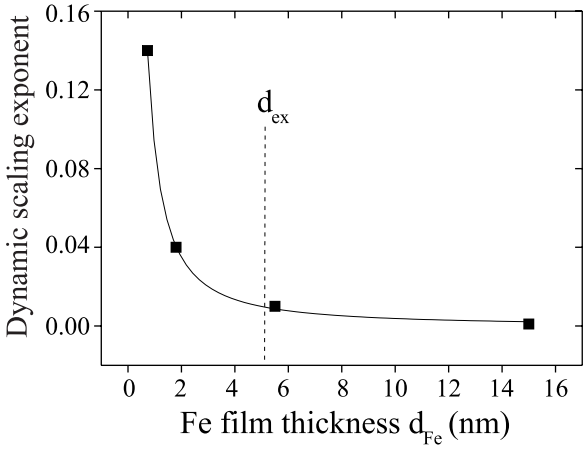

Figure 8. The dynamic scaling exponents α in the low dynamic regime as a function of Fe film thickness for the Fe/GaAs(001) system. The solid curve is a guide to the eye. The exchange length $d_{ex} \approx 50$ Å in Fe.

$\alpha \sim 0.01$), despite the experimental finding that the two systems have contrasting anisotropy strengths and thicknesses. It may thus be concluded that the thickness-dependent anisotropies in these systems do not affect the gradient of H_c^*–f in the low dynamic regime. However, they may affect the height of the energy barrier for domain wall pinning, as reflected in the value of (static or dynamic) coercive field. The dynamic coercive field values across the frequency range in Fe/GaAs(001) are consistently higher than those in Fe/InAs(001), for comparable film thicknesses, indicating a higher energy barrier to reversal in Fe/GaAs(001) that reflects not only interface roughness but also in-plane magneto-crystalline anisotropy strength.

5. Analysis in the context of domain processes

The discrepancy between the predictions of power-law based theoretical models and the results of dynamic hysteresis experiments in thin magnetic films, as detailed in the previous section, has led to a search for models that better fit the experimental data. One such model is the analytical expression of magnetization $M[H, \dot{H}]$ proposed by Raquet *et al*, which accounts for both domain wall motion and nucleation processes, and fits to both low and high dynamic regimes. Our recent work adapts the Raquet model to describe dynamic hysteresis measurements in an empirical manner [56]. The aim of this work was to examine the effect of temperature on the two dynamic regimes. Here, a dip in dynamic coercive field H_c^* for a 150 Å Fe/GaAs(001) film is seen at the crossover from low to high dynamic regime, and the crossover itself shifts to lower sweep rate as the temperature is reduced (figure 9). This latter trend, marked with a dashed line in figure 9, indicates that thermal activation plays a significant role in the reversal dynamics. That the dynamic coercive field decreases with frequency at the crossover before increasing with further increasing frequency suggested that, at two critical frequencies, the applied field changes on two distinct timescales associated with the reversal process, and it was expected that these correspond to a 'wall propagation' timescale τ_p and a 'domain nucleation' timescale τ_n. Using the Raquet idea of competing domain processes at the crossover, the following expression was devised to fit to the experimental data:

$$H_c^* = H_{c,P\to 0}^* \exp\left(\frac{-P}{P_n}\right) + H_c\left(1 - \exp\left(\frac{-P}{P_p}\right)\right). \tag{9}$$

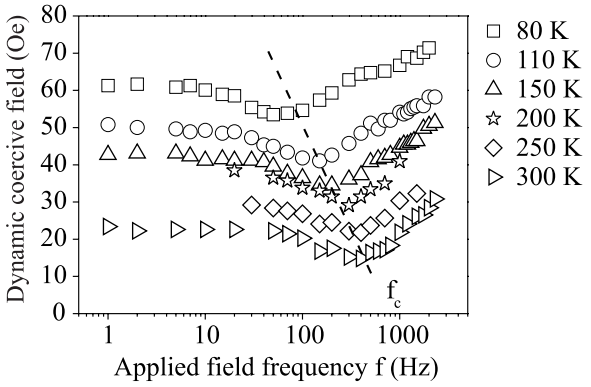

Figure 9. The dynamic coercive field H_c^* as a function of applied field frequency f for 15 nm Fe/GaAs(001) at temperatures in the range 80–300 K. Although H_c^* does increase with falling temperature, as shown, for clarity the datasets are spaced more widely in the vertical direction than is actually the case. The shift of f_c (crossover between low and high dynamic regimes) to lower frequencies with reduction in temperature is highlighted by a dashed line.

Here, P is the drive field period, H_c is the value that H_c^* tends to at high P (the low-frequency coercive field), and $H^*_{c,P\to 0}$ is the value that H_c^* tends to as P tends to zero. P_n and P_p are the critical field periods for nucleation and propagation, respectively. The critical periods correspond to those frequencies where the field begins to be swept fast enough through the coercive field H_c that it changes significantly on the appropriate 'intrinsic' timescale τ_n or τ_p. This can be considered as 'timescale matching' between the sweeping applied field and the nucleation and propagation process. The first term becomes important as P approaches the same order of magnitude as P_n, and controls the onset of the high dynamic regime. The second term becomes important as P approaches the same order of magnitude as P_p, and controls the onset of the dip in H_c^*. The relation between critical periods $P_{n(p)}$ and intrinsic timescales $\tau_{n(p)}$ is not straightforward because it depends on sweep rate which, for a sinusoidal applied field, varies with time.

The assumption in this model is that domain wall propagation dominates the reversal process in the low dynamic regime. Then, as the field begins to be swept fast enough to change during the propagation time τ_p, the domain walls start to be dynamically driven through the film. It was suggested [56] that forced depinning from nucleation sites at these sweep rates gives the dip in coercive field. At still higher sweep rates, the field changes on the nucleation timescale τ_n. This change occurs before the magnetization changes significantly, so beyond the dip the coercive field increases steadily as a function of sweep rate.

Fitting the equation (9) to the experimental data and using the method outlined in [56] allowed the estimation of the timescales τ_n and τ_p, the sum of which corresponded well to measurements of the total switching time.

Our recent study uses time-resolved Kerr magnetometry with a focused laser spot to make real time measurements of the switching in a 50 nm epitaxial Fe/GaAs(001) film as a function of applied sweep rate [57]. In the low dynamic regime, domain walls are observed to jump in a random fashion between pinning sites, whilst in the high dynamic regime the switching is characteristic of field-driven, quasi-continuous wall motion. This study supports the notion of wall propagation-dominated reversal in the low dynamic regime and nucleation-dominated reversal in the high dynamic regime.

Perhaps one of the most comprehensive studies of magnetization reversal dynamics in thin magnetic films is that by Kirilyuk *et al* [58]. One difference between this and the studies on Fe/GaAs(001) is that the Co films investigated have their magnetic anisotropy perpendicular to the film surface. Another difference is that pulsed rather than swept fields were used, although as shown in the introduction the results from these two methods are comparable. Measurements of domain wall velocity and nucleation rate as a function of pulsed field amplitude gave evidence for three different magnetization reversal regimes. At low fields domain wall pinning by structural inhomogeneities controls the thermally activated reversal dynamics, with mean domain wall velocity v proportional to the probability of switching the magnetization in patches:

$$v = v_0 \exp -\left(\frac{E_\mathrm{p} - M_\mathrm{S} V_\mathrm{p} H}{kT}\right). \tag{10}$$

Here, E_p is the propagation energy barrier that depends on temperature and local demagnetizing fields, and V_p is the activation volume of the patch. Above the propagation field value the reversal is dominated by viscous domain wall motion, and the wall velocity may be described by

$$v = v_0 + \mu(H - H_0). \tag{11}$$

This expression applies up to the Walker limit, where the velocity remains constant and varies linearly with magnetic film thickness [59].

The nucleation rate n was consistent with a thermally activated process:

$$n = n_0 \exp -\left(\frac{E_\mathrm{n} - M_\mathrm{S} V_\mathrm{n} H}{kT}\right), \tag{12}$$

where E_n and V_n are the nucleation energy and activation volume, respectively.

The ratio $k \propto n/v$ [6] was found to increase markedly in the high-field regime, indicating that nucleation dominates here. It also suggests that the first two regimes observed in this experiment correspond to the low dynamic regime and high dynamic regime of the swept-field experiments. In fact, both types of experiment can give the same information. The pulsed field technique can give values for activation volumes and energy barriers for both domain nucleation and wall motion processes, if measured data is analysed in the framework of equations (10) and (12). Swept-field measurements are equally useful if analysed with the Raquet expression for field- and sweep rate-dependent magnetization reversal, which is based on the same equations. Of course, in reality the activation volumes and energy barriers are distributed randomly throughout the sample, and the associated statistics of the magnetic switching (e.g. Barkhausen jumps, rate-dependent switching parameter distributions [57, 60–64]) is important for a full understanding of the dynamic hysteresis of thin magnetic films.

6. Dynamic hysteresis in application

Very few works so far have used dynamic hysteresis measurements as a well-known technique for investigating a magnetic film or multilayer. The understanding of dynamic hysteresis has until recently been at a stage where most studies have chosen the simplest possible sample and investigated the different regimes in the dynamic magnetization reversal and the underlying domain processes. However, there are some recent works that have measured more complex samples and used the contemporary knowledge of the physics of dynamic hysteresis to understand the results. For example, Camarero *et al* have studied the magnetization reversal dynamics in exchange-coupled NiO/Co bilayers [65]. Here, the crossover between the low and high dynamic regimes was found to depend on the relative thickness of the NiO

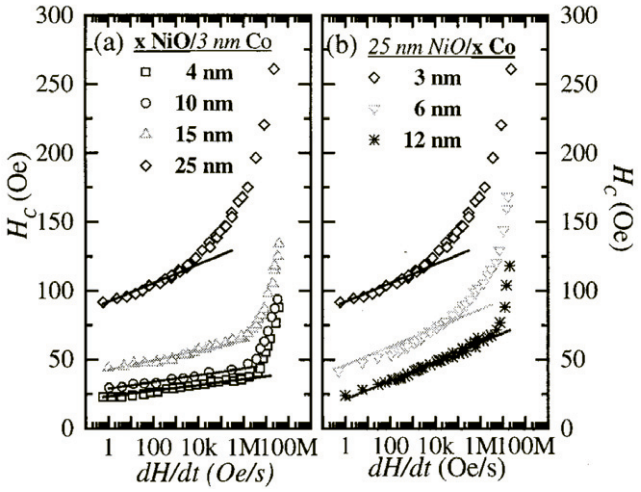

Figure 10. The applied field sweep rate dependence of the coercive field of different exchange-coupled NiO/Co bilayers (from [65]). (a) and (b) show the NiO and Co thickness dependence, respectively. The symbols are experimental data and the lines are fits using equation (7) from [51].

and Co layers: thinner NiO favoured propagation and thinner Co favoured nucleation (see figure 10). Chen *et al* measured dynamic hysteresis loops in superferromagnetic discontinuous $Co_{80}Fe_{20}/Al_2O_3$ multilayers [66] and found a low crossover frequency ($0.05 < f < 1$ Hz) compared to Fe/GaAs(001) (see figure 11). Our recent study of dynamic hysteresis in a continuous Fe/GaAs(001) film patterned with arrays of antidots shows a large difference in coercive field in the crossover region between samples of different antidot density [67]. This result was interpreted in the terms of the adapted Raquet model (equation (9)) as a competition between domain nucleation and wall propagation. Even more recently, Pennec *et al* have imaged by x-ray photoelectron emission microscopy (X-PEEM) the domain structure of the permalloy layer of a spin valve subjected to a varying applied field sweep rate [68]. At low sweep rates one or two reverse domains nucleate and their domain walls propagate, whereas at high sweep rates a large number of reverse domains are created. This confirms experimentally that domain wall motion is dominant in the low dynamic regime, and that domain nucleation is more important in the high dynamic regime.

In this section the work on high speed switching in magnetic recording media [69–72] should be mentioned. These systems are generally treated as assemblies of uniaxial single-domain particles, and are switched using short field pulses. An analysis of Néel thermal activation in a collection of such particles yields the Sharrock equation [19]

$$H_c(t) = H_0\left\{1 - \left[\frac{kT}{KV}\ln\left(\frac{f_0 t}{0.693}\right)\right]^{1/m}\right\}, \tag{13}$$

where t is the demagnetizing time, H_0 the anisotropy field, K the anisotropy constant, V the particle volume, f_0 the attempt frequency ($\sim 10^9$–10^{10} s^{-1}), and the power m takes a value between $3/2$ and 2. This equation predicts a gradual increase of coercive field with decreasing pulse length, and a steep rise in the nanosecond regime, and may be used to fit to coercive field data across the range of accessible experimental timescales t_{exp}. The point to note here is that both the single-domain particles and the continuous films exhibit a crossover from a low dynamic regime (slow increase of coercive field with t_{exp}) to a high dynamic regime

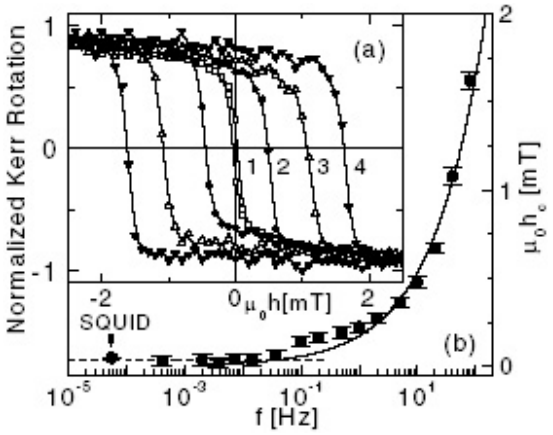

Figure 11. (a) Normalized MOKE loops obtained at $T = 294$ K and $f = 0.002$ (1), 0.1 (2), 10 (3) and 40 Hz (4), and (b) the f dependence of the coercive field (from [66]).

(steep increase of coercive field with t_{exp}), but in different frequency regimes. The crossover occurs when the experimental timescale approaches the timescale of the intrinsic switching process, i.e. coherent rotation on the nanosecond timescale in single-domain particles and domain nucleation/wall propagation on the microsecond timescale in continuous films. As the time of application of the field is reduced, increasingly larger field strength is required to bring the magnetization to zero, to compensate. The equivalent of the Sharrock equation for the switching in continuous films may be provided by the Raquet model [17] or by equation (9).

7. Conclusion

In the mesofrequency range, the magnetization dynamics in thin ferromagnetic films has a richness of character which is only just beginning to be investigated in any detail. The variety of dynamical behaviour for Fe, NiFe and Co films is revealed by the different switching field trends as a function of experimental timescale, $H_S(t_{exp})$. There are two dynamic regimes, the low dynamic regime where the magnetization reversal occurs predominantly by domain wall motion, and the high dynamic regime where domain nucleation is the main reversal process. The high dynamic regime begins at longest t_{exp} in Co thin films, as compared with Fe and NiFe. The intrinsic properties of the material such as the magneto-crystalline anisotropy determine the coercive field and hence t_{exp} at the crossover from low to high dynamic regime. The precise behaviour of the switching field in Fe thin films at the crossover from low to high dynamic regime depends on the competing domain processes of nucleation and wall propagation. In addition, H_S gradually increases with decreasing t_{exp} in the low dynamic regime for films thinner than the exchange length.

We have shown that the measurement of dynamic hysteresis loops by MOKE provides a good method to probe the switching field as a function of experimental timescale in the mesofrequency range (10^{-1}–10^{-6} s) in thin ferromagnetic films. The crucial factor to consider when recording dynamic hysteresis loops is that the photodetector has sufficient bandwidth and response time to capture the fast-changing magnetization. In analysis of the loops, power laws for loop area scaling are generally not relevant in our view because the theoretical models from which they are derived do not consider domain processes. Rather, the Raquet expression for magnetization as a function of applied field and applied field sweep rate, and the empirical

expression (equation (9)) highlighted in this review, fit well to the dynamic coercive field $H_c(f)$ and give physical parameters such as timescales for the processes involved in the mesofrequency reversal dynamics in thin ferromagnetic films. We hope that this review will encourage a wider effort in the experimental and theoretical study of the mesofrequency range of magnetization reversal in thin films.

Acknowledgments

The authors would like to acknowledge the support of the EPSRC (UK) and the Cambridge-MIT Institute.

References

[1] Hillebrands B and Ounadjela K (ed) 2002 *Spin Dynamics in Confined Magnetic Structures I* (*Springer Topics in Applied Physics*) (Berlin: Springer)
[2] Hillebrands B and Ounadjela K (ed) 2003 *Spin Dynamics in Confined Magnetic Structures II* (*Springer Topics in Applied Physics*) (Berlin: Springer)
[3] Kikuchi R 1956 *J. Appl. Phys.* **27** 1352
[4] Ferré J 2002 *Spin Dynamics in Confined Magnetic Structures I* (*Springer Topics in Applied Physics*) (Berlin: Springer) p 127
[5] Zhang G, Hübner W, Beaurepaire E and Bigot J-Y 2002 *Spin Dynamics in Confined Magnetic Structures I* (*Springer Topics in Applied Physics*) (Berlin: Springer) p 245
[6] Labrune M, Andrieu S, Rio F and Bernstein P 1989 *J. Magn. Magn. Mater.* **80** 211
[7] Ferré J, Jamet J P, Pommier J, Beauvillain P, Chappert C, Mégy R and Veillet P 1997 *J. Magn. Magn. Mater.* **174** 77
[8] Silva T J, Lee C S, Crawford T M and Rogers C T 1999 *J. Appl. Phys.* **85** 7849
[9] Freeman M R and Hiebert W K 2002 *Spin Dynamics in Confined Magnetic Structures I* (*Springer Topics in Applied Physics*) (Berlin: Springer) p 93
[10] Russek S E, McMichael R D, Donahue M J and Kaka S 2003 *Spin Dynamics in Confined Magnetic Structures II* (*Springer Topics in Applied Physics*) (Berlin: Springer) p 93
[11] Heinrich B 1994 *Ultrathin Magnetic Structures II* (Berlin: Springer) p 195
[12] Ebels U, Buda L D, Ounadjela K and Wigen P E 2002 *Spin Dynamics in Confined Magnetic Structures I* (*Springer Topics in Applied Physics*) (Berlin: Springer) p 167
[13] Cochran J F 1994 *Ultrathin Magnetic Structures II* (Berlin: Springer) p 222
[14] Demokritov S O and Hillebrands B 2002 *Spin Dynamics in Confined Magnetic Structures I* (*Springer Topics in Applied Physics*) (Berlin: Springer) p 65
[15] Hillebrands B and Ounadjela K (ed) 2003 *Spin Dynamics in Confined Magnetic Structures II* (*Springer Topics in Applied Physics*) (Berlin: Springer) (Preface)
[16] Koopmans B 2003 *Spin Dynamics in Confined Magnetic Structures II* (*Springer Topics in Applied Physics*) (Berlin: Springer) p 253
[17] Raquet B, Mamy R and Ousset J C 1996 *Phys. Rev.* B **54** 4128
[18] Lee W Y, Choi B C, Xu Y B and Bland J A C 1999 *Phys. Rev.* B **60** 10216
[19] Sharrock M P 1990 *IEEE Trans. Magn.* **26** 193
[20] Hatfield W B 1965 *J. Appl. Phys.* **36** 2662
[21] Kryder M H and Humphrey F B 1969 *J. Appl. Phys.* **40** 2469
[22] Atkinson D, Allwood D A, Cooke M D and Cowburn R P 2001 *J. Phys. D: Appl. Phys.* **34** 3019
[23] Choi B C, Belov M, Hiebert W K, Ballentine G E and Freeman M R 2001 *Phys. Rev. Lett.* **86** 728
[24] Gerrits T, van den Berg H A M, Hohlfeld J, Bär L and Rasing T 2002 *Nature* **418** 509
[25] Moore T A, Rothman J, Xu Y B and Bland J A C 2001 *J. Appl. Phys.* **89** 7018
[26] Bozorth R M 1951 *Ferromagnetism* (New York: Van Nostrand-Reinhold)
[27] Smit J and Wijn H P J 1959 *Ferrites* (New York: Wiley)
[28] Ewing J A and Klaassen H G 1893 *Phil. Trans. R. Soc.* A **184** 985
[29] Ewing J A 1900 *Magnetic Induction in Iron and Other Metals* (London: The Electrician)
[30] Steinmetz C P 1892 *Trans. Am. Int. Electr. Eng.* **9** 3
[31] Rayleigh J S W 1887 *Phil. Mag.* **23** 225

[32] Bonfim M, Mackay K, Pizzini S, Arnou M-L, Fontaine A, Ghiringhelli G, Pascarelli S and Neisius T 2000 *J. Appl. Phys.* **87** 5974
[33] Rao M, Krishnamurthy H R and Pandit R 1990 *Phys. Rev.* B **42** 856
[34] Sengupta S, Marathe Y J and Puri S 1992 *Phys. Rev.* B **45** 7828
[35] Dhar D and Thomas P B 1992 *J. Phys. A: Math. Gen.* **25** 4967
[36] Thomas P B and Dhar D 1993 *J. Phys. A: Math. Gen.* **26** 3973
[37] Somoza A M and Desai R C 1993 *Phys. Rev. Lett.* **70** 3279
[38] Zhong F and Zhang J 1995 *Phys. Rev. Lett.* **75** 2027
[39] Lo W S and Pelcovits R A 1990 *Phys. Rev.* A **42** 7471
[40] Luse C N and Zangwill A 1994 *Phys. Rev.* E **50** 224
[41] Acharyya M and Chakrabarti B K 1995 *Phys. Rev.* B **52** 6550
[42] He Y L and Wang G C 1993 *Phys. Rev. Lett.* **70** 2336
[43] Jiang Q, Yang H N and Wang G C 1995 *Phys. Rev.* B **52** 14911
[44] Suen J S and Erskine J L 1997 *Phys. Rev. Lett.* **78** 3567
[45] Suen J S, Lee M H, Teeter G and Erskine J L 1999 *Phys. Rev.* B **59** 4249
[46] Choi B C, Lee W Y, Samad A and Bland J A C 1999 *Phys. Rev.* B **60** 11906
[47] Lee W Y, Xu Y B, Gardiner S M, Choi B C and Bland J A C 2000 *J. Appl. Phys.* **87** 5926
[48] Lee W Y, Samad A, Moore T A and Bland J A C 2000 *Phys. Rev.* B **61** 6811
[49] Lee W Y, Samad A, Moore T A and Bland J A C 2000 *J. Appl. Phys.* **87** 6600
[50] Lee W Y, Choi B C, Lee J, Yao C C, Xu Y B, Hasko D G and Bland J A C 1999 *Appl. Phys. Lett.* **74** 1609
[51] Raquet B, Ortega M D, Goiran M, Fert A R, Redoules J P, Mamy R, Ousset J C, Sdaq A and Khmou A 1995 *J. Magn. Magn. Mater.* **150** L5
[52] Gester M, Daboo C, Hicken R J, Gray S J, Ercole A and Bland J A C 1996 *J. Appl. Phys.* **80** 347
[53] Xu Y B, Kernohan E T M, Freeland D J, Tselepi M, Ercole A and Bland J A C 1999 *J. Magn. Magn. Mater.* **198/199** 703
[54] Xu Y B, Freeland D J, Tselepi M and Bland J A C 2000 *J. Appl. Phys.* **87** 6110
[55] Bruno P, Bayreuther G, Beauvillain P, Chappert C, Lugert G, Renard D, Renard J P and Seiden J 1990 *J. Appl. Phys.* **68** 5759
[56] Moore T A, Wastlbauer G and Bland J A C 2003 *J. Phys.: Condens. Matter* **15** L407
[57] Moore T A, Gardiner S M, Guertler C M and Bland J A C 2004 *Physica* B **343** 337
[58] Kirilyuk A, Ferré J, Grolier V, Jamet J P and Renard D 1997 *J. Magn. Magn. Mater.* **171** 45
[59] Tarasenko S V, Stankiewicz A, Tarasenko V V and Ferré J 1998 *J. Magn. Magn. Mater.* **189** 19
[60] Zapperi S, Cizeau P, Durin G and Stanley H E 1998 *Phys. Rev.* B **58** 6353
[61] Puppin E 2000 *Phys. Rev. Lett.* **84** 5415
[62] Gardiner S M, Rothman J, Xu Y B, Tselepi M, Bland J A C, Cheng Y and Rousseaux F 2001 *J. Appl. Phys.* **89** 6790
[63] Kim D-H, Choe S-B and Shin S-C 2003 *Phys. Rev. Lett.* **90** 087203
[64] Moore T A, Ionescu A and Bland J A C 2004 *J. Appl. Phys.* at press
[65] Camarero J, Pennec Y, Bonfim M, Vogel J, Pizzini S, Fontaine A, Cartier M, Fettar F and Dieny B 2001 *J. Appl. Phys.* **89** 6585
[66] Chen X, Sichelschmidt O, Kleemann W, Petracic O, Binek C, Sousa J B, Cardoso S and Freitas P P 2002 *Phys. Rev. Lett.* **89** 137203
[67] Moore T A, Wastlbauer G, Bland J A C, Cambril E, Natali M, Decanini D and Chen Y 2003 *J. Appl. Phys.* **93** 8746
[68] Pennec Y, Camarero J, Toussaint J C, Pizzini S, Bonfim M, Petroff F, Kuch W, Offi F, Fukumoto K, Nguyen Van Dau F and Vogel J 2004 *Phys. Rev.* B **69** 180402(R)
[69] He L, Doyle W D, Varga L, Fujiwara H and Flanders P J 1996 *J. Magn. Magn. Mater.* **155** 6
[70] Stinnett S M, Doyle W D, Flanders P J and Dawson C 1998 *IEEE Trans. Magn.* **34** 1828
[71] Richter H J, Wu S Z and Malmhäll R 1998 *IEEE Trans. Magn.* **34** 1540
[72] Richter H J and Ranjan R Y 1999 *J. Magn. Magn. Mater.* **193** 213